Multi-band GNSS Front-end Architecture Suitable for Integrated Circuits

Alexander Ruegamer, *Fraunhofer Institute for Integrated Circuits IIS, Nuremberg, Germany*
Santiago Urquijo, *Fraunhofer Institute for Integrated Circuits IIS, Nuremberg, Germany*
Guenter Rohmer, *Fraunhofer Institute for Integrated Circuits IIS, Nuremberg, Germany*

BIOGRAPHY

Alexander Ruegamer received his Dipl.-Ing. (FH) degree in Electrical Engineering from the University of Applied Sciences Wuerzburg-Schweinfurt, Germany in 2007. Since the same year he works at the Fraunhofer Institute for Integrated Circuits IIS in the field of GNSS front-end receiver development with focus on multi-band reception, integrated circuits and immunity to interference.

Santiago Urquijo received the M.Sc. and Ph.D. degrees in Electrical Engineering from the University of Navarra, Spain in 1994 and 2005, respectively. From 1994 to 1997, he worked at the electrical department of the C.E.I.T. where he developed several digital ASICs. In 1997 he was in the analog department of the Fraunhofer Institute for Integrated Circuits IIS as a visiting researcher, returning to San Sebastian as assistant professor. Since 1998, he is member of the navigation group at Fraunhofer IIS in Nuremberg. His main activity domain is currently in the field of mixed analog-digital circuits, signal processing, data converters, and system architecture. He assumes responsibility for the receiver system architecture and implementation of GNSS-systems.

Guenter Rohmer received his Dipl.-Ing. degree in Electrical Engineering in 1988 and the PhD in 1995 from the Technical University of Erlangen, Germany. Since 2001 he is head of a department at the Fraunhofer Institute for Integrated Circuits dealing with the development of components for satellite navigation receivers, indoor navigation and microwave localization systems.

ABSTRACT

This paper introduces a novel multi-band front-end architecture for the new wide-band GNSS signals. It enables the simultaneous reception of both L1/E1 and L5/E5 GPS/ Galileo bands with broad bandwidth. The presented topology is suitable for an integrated circuit implementation. A zero-IF and a low-IF path are combined together which has the advantage of needing only one baseband circuitry and of reducing the number of required components, chip area and power consumption considerably. Moreover only one frequency synthesizer is needed to generate all internal frequencies. The proposed topology and its components are presented. The signal degradation in terms of filtering, quantization and superposition loss of the signal paths is simulated, analyzed and interpreted.

INTRODUCTION

In a few years at least four independent but interoperable global navigation satellite systems (GNSS) will be available: Galileo, GPS III, GLONASS and COMPASS. These new and modernized systems will provide new signals and services. This will be the first time that open service signals will be available worldwide on more than one frequency band. Receivers' performance will be improved by taking advantage of the multi-band navigation:

- Increased accuracy: Multi-band reception enables to measure the ionosphere error and to remove it. The new wide-band signals, especially the Galileo E5 with over 72 MHz bandwidth, promise exceptional multipath resistance and increased tracking accuracy.
- Availability: The interoperability between all GNSS systems increases the availability of the space vehicles from today 24 GPS Navstar and a few GLONASS to over 100 space vehicles with additional Galileo and COMPASS satellites. Both service availability, e.g. in urban canyons, and dilution of precision (DOP) can be improved and therefore also the position accuracy.
- Robustness: If one signal band is malfunctioning, an other one can still be used.
- Integrity: Galileo will provide integrity data within its safety-of-life service in the I/NAV message type broadcasted over E5b-I and E1-B [1]. This service is crucial for many safety critical applications.

When these new GNSS signals will finally be available, several new or enhanced applications will become possi-

ble through the advantages listed above, especially in the mass-market sector. But mass-market applications require small, low power and cheap receiver devices. Therefore an integrated solution is mandatory.

Front-end receivers for these new and nearly all wide-band signals are already available but mostly consist of large, expensive, and high power consuming discrete solutions for professional high-end applications. First integrated multi-band front-end solutions are available, but still improvable.

The proposed receiver architecture does not target the cheapest mass-market sector but rather the advanced mass-market, e.g. the automotive market, where professional high-end receivers would be too expensive, too large and too power consuming but the advantages listed above would bring great improvements or even enable some new applications.

This paper is organized as follows: First the choice of appropriate frequency bands for this receiver type is explained. The second section discusses today's multi-band receivers and their problems concerning their application in the advanced mass-market. The next section describes the proposed architecture. The effects of filtering, analog-to-digital conversion and superposition are quantified, verified via Monte Carlo simulation and discussed before the last section draws conclusions and comments on the advantages of the proposed topology.

FREQUENCY BAND SELECTION FOR AN ADVANCED MASS-MARKET RECEIVER

There are four frequency bands with civil GNSS signals foreseen (see Figure 1): L1 C/A, L1c / E1bc (GPS/Galileo); E6bc (Galileo); L2c (GPS); L5 / E5[ab] (GPS/Galileo). All GNSS signals lie in the protected Radio Navigation Satellite Services (RNSS) band but only the L1/E1 and L5/E5 bands are within the even better protected allocated spectrum for Aeronautical Radio Navigation Services (ARNS). The other two GNSS bands, E6 and L2, only protected through the RNSS, suffer from radar, military transmissions and other potentially strong interferer. [1]

For fast acquisition the relatively narrow-band signals (GPS C/A with BPSK(1) modulation or/and Galileo E1bc with BOC(1,1) modulation) on L1 and E1, respectively, are typically used. The resulting Doppler and chip delay estimation can then be used for high performance tracking with the wide-band L1/E1 MBOC(6,1,1/11), L5/E5a BPSK(10), E5b BPSK(10), or the whole E5 AltBOC(15,10) signals. According to [2] the code measurement noise standard deviation and the multipath code error can be very low especially with Galileo E5 AltBOC(15,10).

To conclude, the Galileo E5 (including the GPS L5, Galileo E5a and E5b) and GPS/Galileo L1/E1 bands are appropriate and selected for an advanced mass-market multi-band GNSS receiver for the following reasons:

- No or only well known interferers, like the DME and TACAN present in E5 band, are expected. Fortunately these pulsed interferences can be mitigated relatively well with pulse blanking strategies, e.g. discussed in [3].
- The signals in the selected bands are appropriate for fast acquisition with the narrow-band L1/E1 signals and for highest tracking accuracy using the wide-band L5/E5 signals.
- Moreover security and safety-of-life related GNSS applications demand an integrity signal, like the one broadcasted over the Galileo E1b and E5b bands.

MULTI-BAND GNSS RECEIVERS TODAY

Four different approaches for multi-band receivers are common today:

There are the discrete high-end front-ends for special applications like GNSS reference receivers [4]. These front-ends provide highest accuracy but are not suited for the intended application due to their high price, very high power consumption and size.

Through the progress made in the field of high-performance analog-to-digital converters (ADC), RF- or sub-sampling ADC front-ends become more and more attractive also for wide-band signals [5],[6]. The desired signals are filtered and then down-converted using intentional aliasing in the analog to digital conversion. This type of architecture requires an extremely low jitter clock and an ADC with a high analog input frequency bandwidth. The sub-sampling architecture has a high power consumption in the front-end and also in the following digital baseband signal processing. Generally this architecture suffers from interferences, aliasing of out-of-band noise into the IF range and potential instability due to the high gain amplification needed within one frequency range. Therefore, the sub-sampling architecture is not appropriate for an integrated advanced mass-market receiver.

Another way multi-band reception can be provided is by using separate single frequency front-ends for every desired GNSS signal or by integrating several more or less stand alone receivers on one single chip [7]. This is the straight forward way but it suffers from self-made interferences through the different frequency synthesizers needed and is not an economic nor an optimized solution in terms of power consumption and size.

Other fully integrated multi-band front-end architecture solutions proposed in [8] and [9] use a switch for band selection. Therefore, they can only receive one single band at a time, loosing the advantages of simultaneous multi-frequency GNSS processing such as ionosphere correction.

A new front-end architecture with simultaneous multi-band reception is proposed in this paper where as many receiver

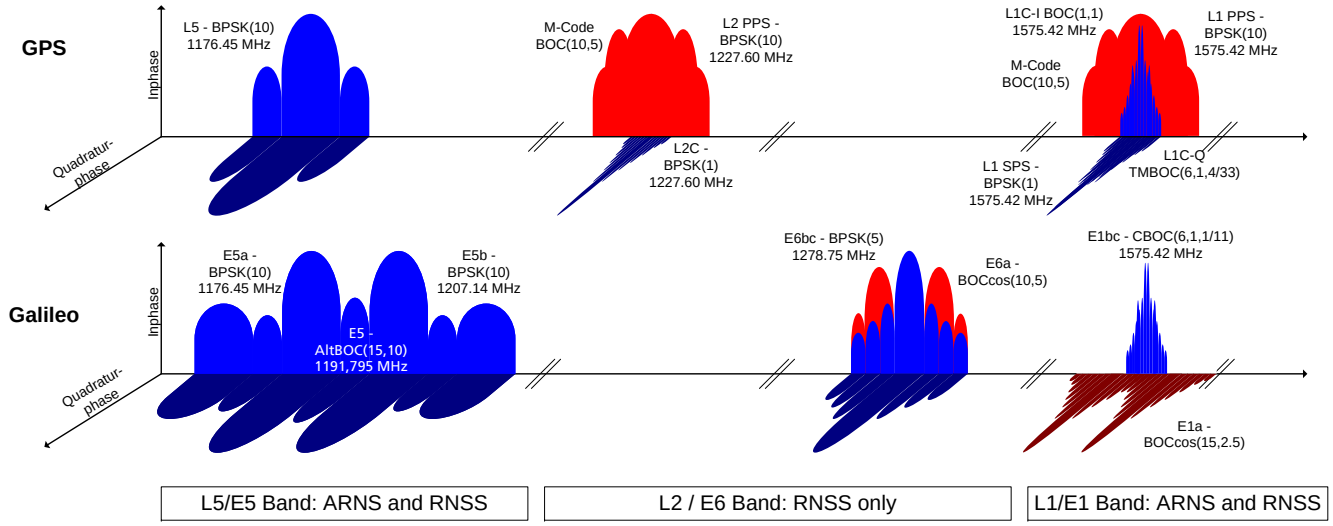

Figure 1. GPS and Galileo signals

blocks in the architecture are shared as long as it is sensible. This architecture is therefore efficient in terms of cost, size and power consumption with simultaneous reception of the broadband Galileo E5, E1 and GPS L5, L1 bands while being suitable for integrated circuit solutions.

PROPOSED ARCHITECTURE

The upcoming Galileo and GPS signals are wide-band, with a bandwidth of around 14 MHz for MBOC(6,1,1/11) modulated signals in L1/E1 and over 72 MHz for the Galileo AltBOC(15,10) modulated signal in E5. Larger bandwidths imply an increase of the power consumption which is problematic especially in portable devices.

In order to achieve low power consumption, it is recommended to reduce the sampling frequency of the ADC as much as possible. According to Nyquist's theorem, the sampling frequency should be at least twice the highest frequency to be digitized. Therefore, the minimum possible Galileo E5 AltBOC(15,10) sampling frequency for today's widespread low-IF GNSS front-end receivers must be at least 144 MHz. A zero-IF topology instead considerably relaxes the sampling frequency, since only a sampling frequency of about 72 MHz is required. However, a zero-IF topology requires two ADCs for the in-phase and the quadrature components in order to reconstruct the complex signal in the digital domain. The zero-IF architecture eliminates the image problem and simplifies the channel selection filtering with a low-pass filter. Therefore, the zero-IF topology is appropriate for receiving the complete Galileo E5 signal.

The presented architecture, depicted in Figure 2, consists of a zero-IF down-conversion path for the L5/E5 bands and a double heterodyne low-IF path for the L1/E1 bands.

An external active antenna with appropriate amplification is assumed. The L1/E1 and E5 RF channel filters can be located within the active antenna or on the front-end printed circuit board (PCB). An external reference frequency element, e.g. a TCXO, is also needed on the PCB. The rest of the depicted architecture blocks can be completely realized on-chip, in a single integrated circuit.

E5 path

The incoming E5 signal, amplified and filtered in the active antenna, is amplified again and directly shifted to baseband by a quadrature down-conversion mixer, as shown in the *E5 Path* frame of Figure 2. A high-pass filter in both in-phase and quadrature component branches is used to eliminate the typical zero-IF problems like 1/f- or flicker-noise (especially important in RF-CMOS technologies), self-mixing and DC-offset. Although the high-pass filter reduces signal energy around the zero-frequency, it does not degrade the reception performance significantly as shown by simulations later on.

E1 path

Like the E5 signal, the incoming L1/E1 signal is amplified and filtered in the active antenna. After the on-chip LNA, the L1/E1 signal is down-converted to a low-IF via two steps, see the *E1 Path* frame of Figure 2. A double heterodyne architecture is selected for the L1/E1 reception path to circumvent the image problem of a pure low-IF architecture. The first and second IF frequencies are approximately 383 MHz and -14 MHz. The image frequency is sufficiently attenuated by the external RF channel filter, e.g. through a 14 MHz band-pass SAW filter in the active antenna. No power and area consuming polyphase filters are needed.

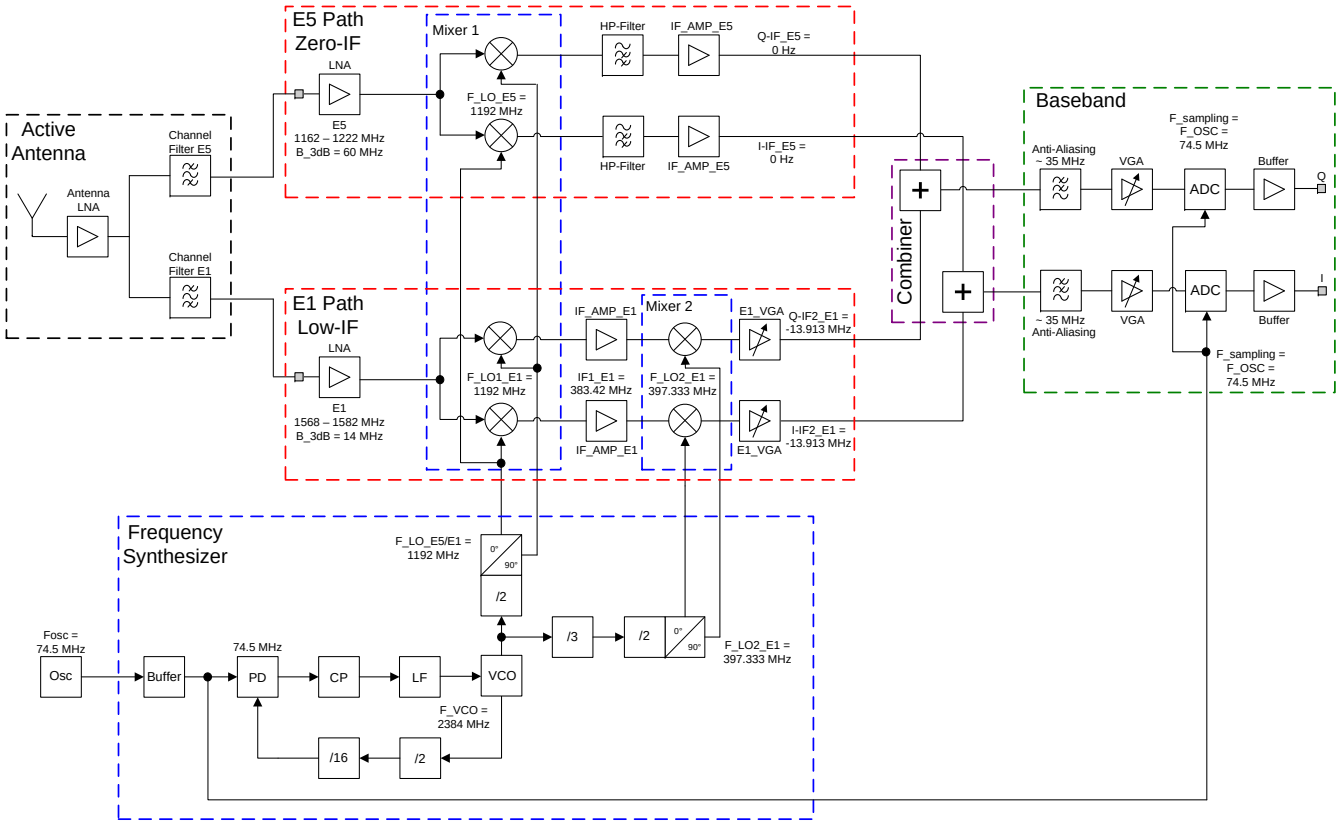

Figure 2. Proposed multi-band front-end architecture

Table 1. Possible reference oscillator frequencies (Fosc) and the resulting local oscillator (LO) and intermediate frequencies (IF), all frequencies in MHz

Ref. Osc. multi-by-16	Ref. Osc. multi-by-32	Ref. Osc. multi-by-64	E5 center freq. 1191.795 MHz		E1 center freq. 1575.42 MHz $LO_{E5/E1_1}$ div-by-3		
ADC			$LO_{E5/E1_1}$	IF_{E5}	IF_{E1_1}	LO_{E1_2}	IF_{E1_2}
74.175	37.087	18.544	1186.795	5.000	388.625	395.598	-6.973
74.237	37.119	18.559	1187.795	4.000	387.625	395.932	-8.307
74.300	37.150	18.575	1188.795	3.000	386.625	396.265	-9.640
74.362	37.181	18.591	1189.795	2.000	385.625	396.598	-10.973
74.425	37.212	18.606	1190.795	1.000	384.625	396.932	-12.307
74.487	37.244	18.622	1191.795	0.000	383.625	397.265	-13.640
74.500	**37.250**	**18.625**	**1192.000**	**-0.205**	**383.420**	**397.333**	**-13.913**
74.550	37.275	18.637	1192.795	-1.000	382.625	397.598	-14.973
74.612	37.306	18.653	1193.795	-2.000	381.625	397.932	-16.307
74.675	37.337	18.669	1194.795	-3.000	380.625	398.265	-17.640
74.737	37.369	18.684	1195.795	-4.000	379.625	398.598	-18.973
74.800	37.400	18.700	1196.795	-5.000	378.625	398.932	-20.307

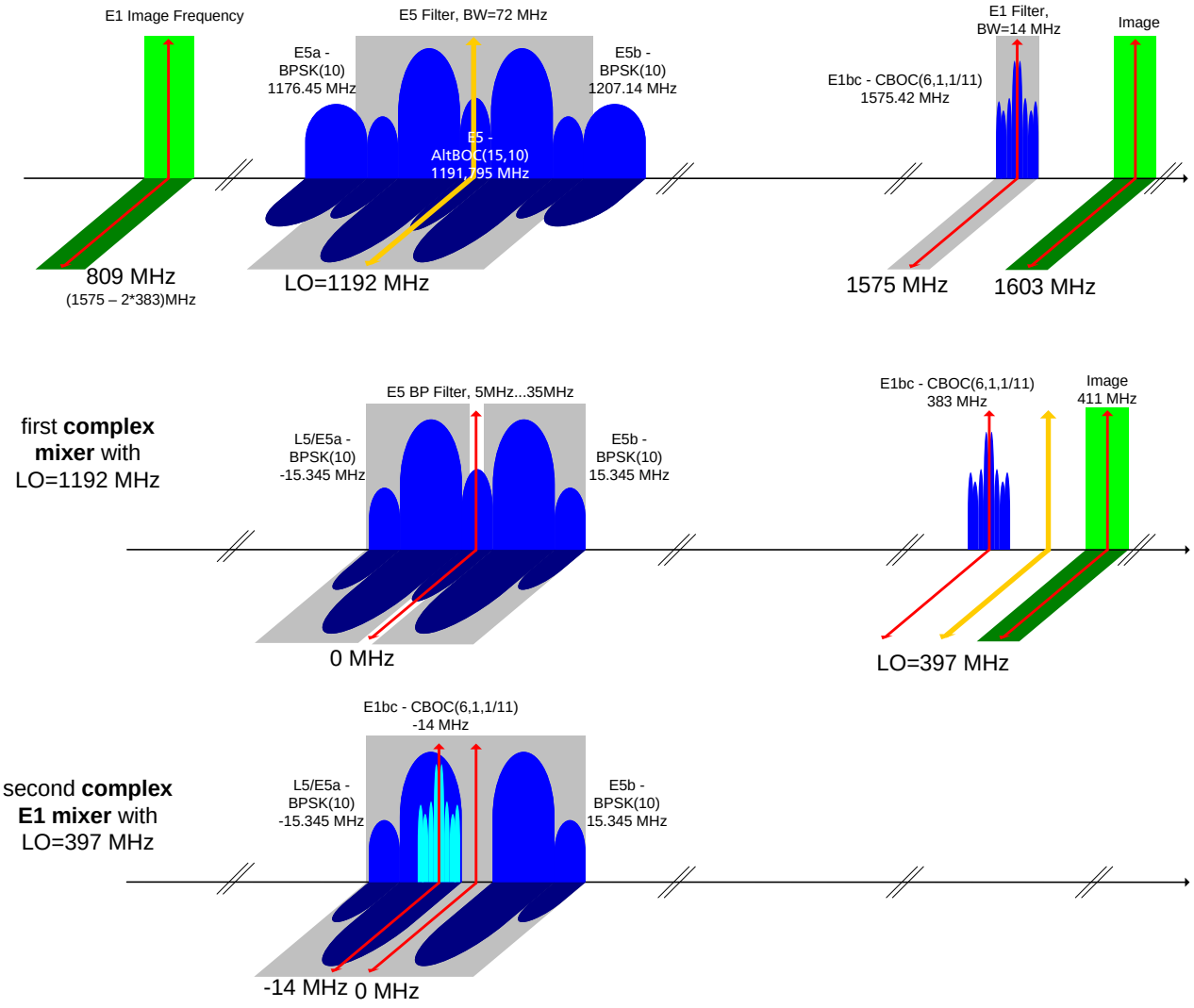

Figure 3. Signals down-conversion and their intermediate frequencies

Table 2. GNSS signals received with their corresponding bandwidths and intermediate frequencies (IF)

GNSS Signal	Carrier Frequency [MHz]	Modulation	RX Band-width [MHz]	IF [MHz]
GPS L1 C/A	1575.42	BPSK(1)	14	-13.913
GPS L1c	1575.42	TMBOC(6,1,4/33)	14	-13.913
Galileo E1bc	1575.42	CBOC(6,1,1/11)	14	-13.913
Galileo E5	1191.795	AltBOC(15,10)	70	-0.205
Galileo E5a	1176.45	BPSK(10)	32	-15.55
GPS L5	1176.45	BPSK(10)	32	-15.55
Galileo E5b	1207.14	BPSK(10)	32	+15.14

Frequency synthesizer

All necessary frequencies for the mixers and ADC can be obtained from the same unique frequency synthesizer. With the presented frequency plan (see Figure 3 and Table 1), the chosen integer-N synthesizer implementation reduces the circuitry complexity and the power consumption.

The high phase detector (PD) frequency (74.5 MHz) enables the on-chip integration of the loop-filter (LF), which reduces the number of off-chip components. Therefore, all phase-locked loop (PLL) components can be integrated on-chip.

The digital frequency dividers can be realized using highly integrated and low-power consuming current mode logic (CML). The divide-by-2 blocks are used for the I/Q generation and one divide-by-3 block is needed for the L1/E1 "Mixer 2" local oscillator (LO) frequency generation.

In this particular example a reference clock oscillator frequency (Fosc) of 74.5 MHz is used. The topology accepts also higher and lower clock frequencies. However, to preserve the advantages of a low complexity and low power consuming integer-N PLL only a relatively narrow range of possible reference oscillator frequencies can be used. Reference frequency values between 74.175 and 74.800 MHz shift the baseband IF frequency of the E5 "zero-IF" path from -5 MHz to +5 MHz. This range is acceptable since only negligible signal power of the E5 AltBOC(15,10) modulated signal is present there. If the E5 LO frequency is changed through the reference frequency, the E1 IF frequencies change too, since they are directly derived from this E5 LO frequency (see Table 1).

A reference frequency lower than half the sampling frequency leads to reference spurs in the baseband range which is converted to the digital domain. These spurs are produced from the integer-N PLL. To avoid these self-made interferences, a reference frequency higher than the anti-aliasing cut-off frequency is recommended. Therefore, the 74 MHz and 37 MHz values in Table 1 are the preferred choice.

Combiner and baseband

All received GNSS signals are code division multiple access (CDMA) based signals with a negative signal to noise ratio (SNR) before the correlation. As shown by simulation results in the next section, the two paths can be combined together with acceptable signal degradation due to the superposition. The baseband part, which is common for the overlapped L1/E1 and L5/E5 bands, consists of two anti-aliasing low-pass filters, an automatic power control realized with two variable gain amplifiers (VGA) and two ADCs for in-phase and quadrature processing. This considerably reduces the required chip area, pins and power consumption.

To minimize the SNR degradation due to superposition of both paths the power levels of these paths must be set correctly. As shown in the next section, when both paths are equally amplified, the combination increases the noise floor and decreases, therefore, the SNR of E1 by 3 dB. At the same time, the noise floor of the E5 signal is only increased by about 0.9 dB due to the smaller filtered E1 bandwidth. The E5b signal, located at +15.55 MHz IF is not affected at all if the E1 filter has adequate stop-band attenuation.

An additional variable gain amplifier is needed in at least one path to be able to control the noise floor power and thus the degradation between L1/E1, E5 and L5/E5a signals, respectively. A noise floor calibration can be performed initially or any time the digital control algorithm requests it. One possible calibration method can be implemented in the digital domain by measuring the noise variance of each path independently when the other one is switched off. When both variances are known, the gain correction can be set appropriately.

When only one signal path is needed, e.g. the L1/E1 GPS/Galileo during the acquisition phase, the other path can be turned off. The SNR degradation due to the increment of the noise floor and the power consumption of the unused path will be eliminated. This helps in degraded signal environments and can also be regarded as an energy saving mode. In the subsequent tracking phase when both bands are used, the SNR degradation between L1/E1 and E5/E5a/L5 can be controlled with an additional VGA (e.g. the E1_VGA in Figure 3).

ANALYSIS OF SIGNAL DEGRADATION EFFECTS

In this section the relevant front-end effects for this architecture type are analyzed. First the effects of low- and high-pass filtering are studied. Then, the losses due to analog-to-digital conversion and superposition are quantified. Finally a Monte Carlo simulation is used to verify the architecture and the results stated before.

Power spectral densities of AltBOC and BOCsin signals

The power spectral density (PSD) describes the power distribution over the frequency. The normalized analytical continuous PSDs for Galileo's E5 alternate binary offset carrier (AltBOC) and BOCsin signals can be found in [10] and [11]. They are used for the following filter losses evaluation and spectral separation coefficients calculation.

The normalized Galileo E5 AltBOC(15,10) PSD for odd $2f_s/f_c$ ratio is given by

$$S_{\mathrm{AltBOC}(f_s,f_c)}(f) = \frac{f_c}{2\pi^2 f^2} \cdot \frac{\cos^2(\frac{\pi f}{f_c})}{\cos^2\left(\frac{\pi f}{3f_c}\right)} \cdot \left[\cos^2\left(\frac{\pi\, f}{2\, f_s}\right) - \cos\left(\frac{\pi\, f}{2\, f_s}\right) - 2\cos\left(\frac{\pi\, f}{2\, f_s}\right)\cos\left(\frac{\pi\, f}{4\, f_s}\right) + 2\right] \quad (1)$$

with f_s being the sub-carrier rate of 15.345 MHz and f_c being the chipping rate of 10.230 MHz.

The normalized BOCsin PSD for even $2f_s/f_c$ ratio is given by

$$S_{\mathrm{BOCsin}(f_s,f_c)}(f) = \frac{1}{f_c}\mathrm{sinc}^2\left(\frac{\pi f}{f_c}\right)\tan^2\left(\frac{\pi f}{2f_s}\right) \quad (2)$$

using a chipping rate f_c of 1.023 MHz and a sub-carrier rate f_s of 1.023 MHz for BOCsin(1,1) and 6.138 MHz for BOCsin(6,1), respectively.

The multiplexed binary offset carrier (MBOC) modulation, implemented as composite BOC (CBOC) for Galileo E1bc and time-multiplexed BOC (TMBOC) for GPS L1c, is defined in the spectrum and therefore also its PSD is defined as follows:

$$S_{\mathrm{MBOC}(6,1,1/11)}(f) = \frac{10}{11}S_{\mathrm{BOCsin}(1,1)}(f) + \frac{1}{11}S_{\mathrm{BOCsin}(6,1)}(f) \quad (3)$$

Filter losses

Using these analytical and continuous PSD expressions, the signal loss due to filtering can be evaluated.

The cut-off frequency plotted in Figures 4 and 5 is the equivalent complex low-pass bandwidth which is half the RF band-pass bandwidth. Since the Galileo Open Service ICD gives no specification of the transmitted bandwidth, the signal filtering losses were simulated for three different transmission bandwidths: unlimited, probable (according to IfEN NCS signal generator's transmitted bandwidth [12]) and minimum required receiver bandwidth (according to Galileo's Open Service ICD [1]).

Figure 4 shows the filter loss results of an ideal complex low-pass filter with varying cut-off frequency for the MBOC signals, using Equation 3. Due to the E1 RF band-pass filter of around 14 MHz (equivalent to 7 MHz complex low-pass bandwidth) a filter loss of around 0.27 dB occurs for unlimited transmission bandwidth, 0.17 dB for 40.92 MHz (NCS signal generator) and 0.09 dB for 24.552 MHz, the E1 Galileo receiver reference bandwidth according to [1].

In contrast to the E1 signal where the filter loss mainly originates from the external RF filter, the E5 AltBOC(15,10) filter loss of the zero-IF path comes from the anti-aliasing low-pass filter and the DC and 1/f-noise removing high-pass filter.

The anti-aliasing low-pass filter bandwidth of the proposed architecture is 35 MHz. Through the slowly decreasing signal power of the AltBOC modulation, the theoretical power loss due to low-pass filtering strongly depends on the transmitted E5 bandwidth.

With 51.150 MHz transmitted E5 bandwidth (minimum receiver bandwidth according to [1], including only the two main-lobes), no additional E5 filter loss occurs. 90.07 MHz

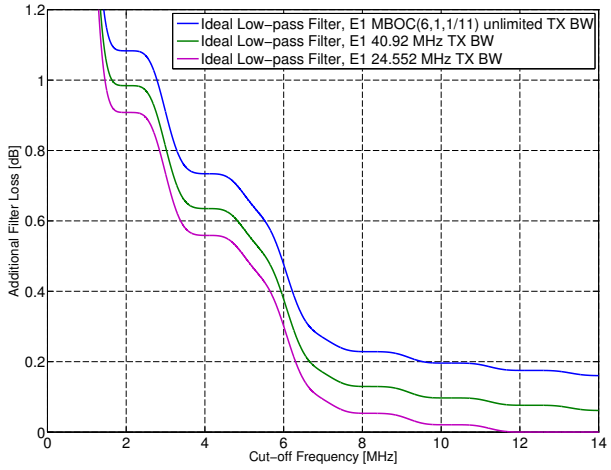

Figure 4. L1/E1 MBOC(6,1,1/11) filter loss with ideal low-pass for different transmission bandwidths

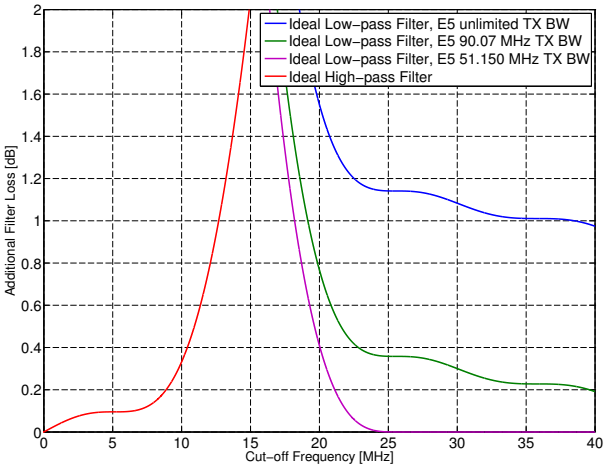

Figure 5. E5 AltBOC(15,10) filter loss with ideal low- and high-pass filter for different transmission bandwidths

transmitted bandwidth (limited transmitted bandwidth according to [12], including both side-lobes next to the main-lobes) leads to 0.23 dB filter loss and slightly more than 1 dB filter loss occurs if no transmitted bandwidth limitation through the space vehicle filter would be applied.

The high-pass filter in the E5 path is used to eliminate DC-offset, self-modulation and 1/f-noise effects. Especially important in RF-CMOS technologies is the 1/f noise with a corner frequency in the order of 0.1-1 MHz [13]. Therefore a high-pass filter with at least this cut-off frequency should be used. Figure 5 shows that even a high-pass cut-off frequency of around 5 MHz leads only to an additional filter loss of less than 0.1 dB.

The ideal brick-wall filtered baseband signals with the same normalized power levels before filtering are depicted on their IFs in Figure 6. One can clearly see that only the left main-lobe of E5 (equal to Galileo E5a and GPS L5)

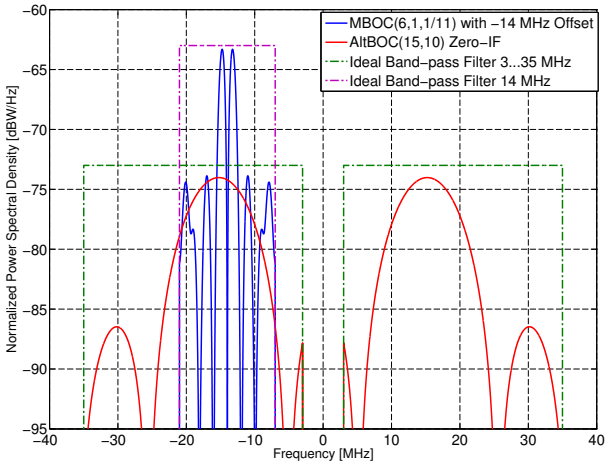

Figure 6. Filtered baseband signals, Galileo E5 and E1

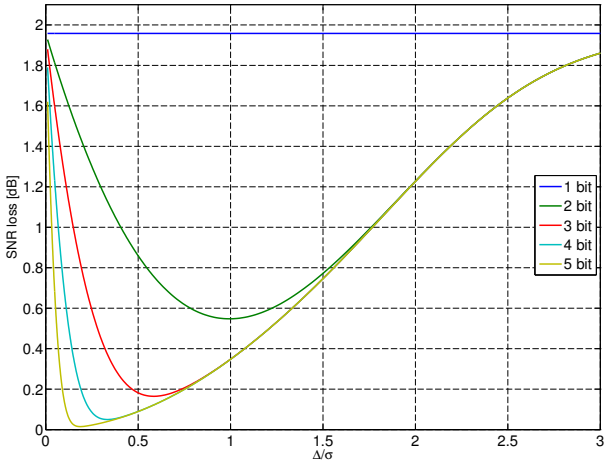

Figure 7. n-bit ADC implementation loss

is affected by the superposition. The right main-lobe comprising Galileo E5b remains untouched.

ADC implementation loss

The ADC implementation loss is depicted in Figure 7. The degradation depends on the ADC resolution and the ADC control through an automatic power or gain control. The x-axis gives the ratio between the ADC threshold Δ and the standard deviation σ of the normally distributed input signal. A 3-bit ADC is a good trade-off between complexity and power consumption. It has a low implementation loss and achieves a large dynamic range, which is required in presents of interference. An optimally controlled 3-bit ADC leads to 0.17 dB implementation loss if only white Gaussian noise is present which is a reasonable assumption under normal operating conditions.

Spectral separation coefficients

The spectral separation coefficient (SSC) can be used to quantify the interference between two signals. SSC measures how orthogonal two signals are. If the PSDs do not overlap, e.g. are separated through distant frequency bands, the SSC approaches zero. The PSDs of BOCsin, MBOC and AltBOC signals are given in equations 2, 3 and 1. They are all normalized to unity over infinite bandwidth. According to [14], the SSC can be computed with

$$\mathrm{SSC} = \int_{-\infty}^{\infty} S_s(f)\, S_i(f)\, df \tag{4}$$

For our case this equation is modified and extended with a frequency shift to consider the different baseband IFs and with filters. The filter characteristics of the 3 MHz high-pass and 35 MHz low-pass filter ($|H_s|^2$) for E5 AltBOC and the 14 MHz band-pass filter characteristic ($|H_i|^2$) for the E1 MBOC signal are used. Thus, the SSC is computed as follows:

$$\mathrm{SSC} = \int_{-\infty}^{\infty} |H_s|^2 S_s(f+f_{IF_s})\, |H_i|^2 S_i(f+f_{IF_i})\, df \tag{5}$$

The results of Equation 5 are shown in Table 3 for different signal superposition combinations. MBOC or AltBOC are the unlimited PSDs. The filtered versions include a 7 MHz low-pass for MBOC and a 3 to 35 MHz band-pass for AltBOC. The IF indices indicate the shift of the MBOC PSD to the IF frequency of -14 MHz. The SSC of $\mathrm{MBOC}_{\mathrm{filtered,IF}}$ with $\mathrm{AltBOC}_{\mathrm{filtered}}$ is -74.93 dB/Hz. Compared to the self-interferences of $\mathrm{AltBOC}_{\mathrm{filtered}}$ with -76.59 dB/Hz, the superposition is only slightly worse. The $\mathrm{MBOC}_{\mathrm{filtered}}$ self-interference is -65.66 dB/Hz so the superposition SSC is 9.27 dB better. The lowest spectral separation coefficient is given for $\mathrm{AltBOC}_{\mathrm{filtered}}$ and $\mathrm{MBOC}_{\mathrm{filtered}}$ with -93.67 dB/Hz, because in that configuration the PSDs hardly overlap. So this would be the most desired combination, but such an IF concept is not possible without using a much more complicated frequency synthesizer as the one proposed in this paper.

Superposition loss and noise

Using these SSC values, the effective C/N_0 can be calculated according to [14]:

$$\frac{C_s}{N_{0\,\mathrm{eff}}} = \frac{C_s}{N_0} \frac{\int |H_s|^2\, S_s(f)\, df}{\int |H_s|^2\, S_s(f)\, df + \frac{C_i}{N_0}\,\mathrm{SSC}} \tag{6}$$

Now the SNR degradation can be determined with:

$$\mathrm{SNR}_{\mathrm{loss}} = \frac{C_s/N_0}{C_s/N_{0_{\mathrm{eff}}}} = 1 + \frac{C_i}{N_0} \frac{\mathrm{SSC}}{\int |H_s|^2\, S_s(f)\, df} \tag{7}$$

In this case, with a SSC of about -75 dB/Hz and a realistic C_i/N_0 operating range between 20 and 45 dBHz, the superposition effect between the signals is negligible (below 0.01 dB of SNR loss). But this SNR superposition loss does not take into account the impact of the additional noise introduced by the combination of two paths.

Table 3. Spectral separation coefficients (SSC) for different signal superpositions, in [dB/Hz]

	MBOC	$\text{MBOC}_{\text{filtered}}$	MBOC_{IF}	$\text{MBOC}_{\text{filtered,IF}}$	AltBOC	$\text{AltBOC}_{\text{filtered}}$
MBOC	-65.66	-65.66	-86.90	-87.55	-84.04	-90.54
$\text{MBOC}_{\text{filtered}}$	-	-65.66	-87.55	-88.29	-84.59	**-93.67**
MBOC_{IF}	-	-	-65.66	-65.66	-74.91	-74.91
$\text{MBOC}_{\text{filtered,IF}}$	-	-	-	-65.66	-74.93	**-74.93**
AltBOC	-	-	-	-	-76.51	-76.59
$\text{AltBOC}_{\text{filtered}}$	-	-	-	-	-	-76.59

The noise bandwidth within E5 is 64 MHz (-35 to -3 MHz and +3 to +35 MHz). The E1 noise bandwidth is 14 MHz (-7 to +7 MHz). The combiner does not only add the signals, but also their noise floors. The increased noise-floor (superposition noise) for E5 is

$$\Delta_{E5} = 10\log_{10}\left(\frac{BW_{E5} + BW_{E1}\cdot \text{VGA}_{\text{E1}}}{BW_{E5}}\right) \quad (8)$$

and the superposition noise for E1 is

$$\Delta_{E1} = 10\log_{10}\left(\frac{BW_{E5}|H_{14\,\text{MHz}}|^2 + BW_{E1}\cdot \text{VGA}_{\text{E1}}}{BW_{E1}\cdot \text{VGA}_{\text{E1}}}\right) \quad (9)$$

Under the assumption that the SNR and the amplification is the same for the E1 and E5 paths, and no E1 VGA is present ($\text{VGA}_{\text{E1}} = 0$ dB, see also Figure 2), the filtered E1 signal with 14 MHz bandwidth gets all of the noise from the E5 path within its bandwidth. The SNR degradation of 3.01 dB for the E1 signal is obvious, since the noise-floor within the E1 bandwidth is doubled. The noise within the wide-band E5 signal is only increased on the E5a signal where the E1 IF signal overlaps. Therefore, the SNR degradation of 0.86 dB for the complete E5 signal is much lower. The degradation for the GPS L5 or the Galileo E5a signal, respectively, within -35 to -3 MHz bandwidth is 1.58 dB. There is no superposition noise degradation at all for the Galileo E5b signal.

With the help of a variable gain amplifier in one or in both of the signal paths the superposition noise can be adjusted. This is depicted in Figure 8 for an E1 VGA present in the E1 path, as depicted in Figure 2. When using both paths simultaneously the minimal superposition noise loss for E1 and E5 signals is 1.67 dB with setting the E1 VGA to 3.3 dB gain. The minimal superposition noise loss for E1 and L5/E5a signals is 2.21 dB with setting the E1 VGA to 1.8 dB gain.

Monte Carlo simulation of the named effects

A Monte Carlo simulation was used to verify the theoretical losses and considerations made above. The receiver chain was simulated with 1000 iterations with a SNR of -36.6 dB which corresponds to a C/N0 of 41.5 dBHz for E5 and 34.9 dBHz for E1, respectively, to be consistent with the superposition noise assumptions made before. Table 4 summarizes the results.

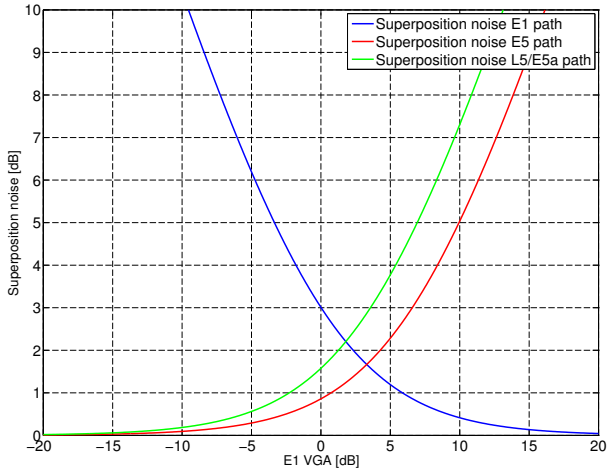

Figure 8. Superposition noise loss adjustable with a VGA (here with one E1 path VGA)

The results match the predicted values well. Only the filter losses are higher than expected for both E1 and E5. If the SNR is set to a high positive value in the Monte Carlo simulation the filter losses match the predicted values perfectly. For the ideal filter loss evaluations (Figures 4 and 5) no noise was considered. In the Monte Carlo simulation used for Table 4 the noise is dominant (SNR=-36.6 dB) and is not completely removed within the correlation. Therefore, higher losses are noticeable.

Unregarded degradation effects

For determination of the overall front-end SNR loss some additional effects would have to be considered. They were not discussed here since they are not specific to the proposed architecture.

E.g. the front-end noise figure has a great impact. This important parameter has not been discussed because it is mainly set by the parameter of the active antenna LNA according to Friis's formula. Further front-end related contributions like phase noise and I/Q amplitude/phase mismatch were neglected since their impact is typically low and have no particular effect within the proposed architecture.

The values in Table 4 give a good idea of how important the influences of the different SNR degradation sources are. In reality the filter losses will be different because analog filters have considerably worse parameters than the ideal

Table 4. Theoretical and Monte Carlo (MC) simulated losses

	E1 MBOC, 14 MHz			E5 AltBOC, 3 to 35 MHz		
	theory	MC simulation mean (μ)	MC simulation std (σ)	theory	MC simulation mean (μ)	MC simulation std (σ)
LP filter loss [dB]	0.17	0.34	0.02	0.23	0.68	0.07
HP filter loss [dB]	-	-	-	0.10		
ADC 3 bit loss [dB]	0.17	0.17	0.04	0.17	0.18	0.26
Superposition loss [dB]	0.01	3.05	0.40	0.01	0.90	0.61
Superposition noise [dB]	3.01			0.81		
Overall SNR loss [dB]	3.36	3.56	0.40	1.32	1.76	0.67

brick wall filters used here. Additionally the ADC implementation loss assumption (only white Gaussian noise at the input) is not given anymore, since the input noise is filtered and therefore no longer white. Finally, all examined degradation effects are more or less correlated. Further investigations taking these effects into account are subject for future work.

CONCLUSIONS

The proposed front-end architecture enables the simultaneous reception of the Galileo E1/E5 and GPS L1/L5 signals with broad bandwidth. By using the presented frequency plan with only one frequency synthesizer and sharing the baseband parts with a superposition concept, this architecture is efficient in terms of cost, size and power consumption and therefore suited for an integrated circuit. The effects of filter loss, ADC implementation loss and superposition loss were analyzed theoretically and verified by Monte Carlo simulation. It was shown that the SNR degradation through the superposition is small compared to the savings enabled by this type of receiver architecture. Moreover, the superposition degradation can be controlled by using a variable gain element in at least one signal path.

ACKNOWLEDGMENTS

This work was supported by a Fraunhofer IIS internal research program (IIFOP). The authors express their appreciations to all members of this project.

REFERENCES

[1] "Galileo Open Service Signal In Space Interface Control Document (OS SIS ICD), Draft 1," tech. rep., European Space Agency/European GNSS Supervisory Authority, February 2008.

[2] J.-M. Sleewaegen, W. De Wilde, and M. Hollreiser, "Galileo AltBOC Receiver," in *Proc. of ENC-GNSS 2004, Rotterdam*, 2004.

[3] G. X. Gao, "DME/TACAN Interference and its Mitigation in L5/E5 Bands," in *ION GNSS 20th International Technical Meeting of the Satellite Division, 25-28, September 2007, Fort Worth, TX*, 2007.

[4] F. Foerster, A. Carrera, N. Lucas, and G. Rohmer, "High Performance Receiver Front-End for Multiple Galileo Frequencies," in *Proceedings of the 18th International Technical Meeting of the Satellite Division of the Institute of Navigation ION GNSS 2005*, pp. 935 – 940, Sep. 2005.

[5] A. Alonso, J.-M. Perre, and I. Arizaga, "A Direct Sampling Digital Receiver For Multiple GNSS Signals," in *Proc. of ENC-GNSS 2008*, 2008.

[6] E. R. Parada, F. Chastellain, C. Botteron, Y. Tawk, and P.-A. Farine, "Design of a GPS and Galileo Multi-Frequency Front-End," in *IEEE 69th Vehicular Technology Conference: VTC2009-Spring 26-29 April 2009, Barcelona, Spain*, 2009.

[7] Z. Gradincic, "Multiband GNSS Receiver," 2007. US20070096980 A1.

[8] M. Detratti, E. Lopez, E. Perez, and R. Palacio, "Dual-Band RF Front-End Solution for Hybrid Galileo/GPS Mass Market Receivers," in *Consumer Communications and Networking Conference, 2008. CCNC 2008. 5th IEEE*, pp. 603–607, Jan. 2008.

[9] J. Ko, J. Kim, S. Cho, and K. Lee, "A 19-mW 2.6-mm2 L1/L2 dual-band CMOS GPS receiver," *Solid-State Circuits, IEEE Journal of*, vol. 40, pp. 1414–1425, July 2005.

[10] J. V. P. Gisbert, "Interference assessment using up to date public information of operating and under development RNSS systems," in *4th European Workshop on GNSS Signals and Signal Processing GNSS Signals 2009*, 2009.

[11] E. Rebeyrol, C. Macabiau, L. Lestarquit, L. Riesa, J.-L. Issler, M.-L. Boucheret, and M. Bousquet, "BOC Power Spectrum Densities," in *Proceedings of the 2005 National Technical Meeting of the Institute of Navigation*, 2005.

[12] IfEN GmbH, "NAVX-NCS Navigation Constellation Simulator Data Sheet," 2009.

[13] F. Ellinger, *Radio Frequency Integrated Circuits and Technologies*. Springer, 2007.

[14] E. D. Kaplan and C. J. Hegarty, *Understanding GPS: Principles and Applications, Second Edition*. Artech House, 2006.